Heliyon 6 (2020) e04239

Contents lists available at ScienceDirect

Heliyon

journal homepage: www.cell.com/heliyon

Research article

Chemical reactivity and bioactivity properties of pyrazinamide analogs of acetylsalicylic acid and salicylic acid using conceptual density functional theory

Al Rey Villagracia [a,*], Hui Lin Ong [b,d], Faith Marie Lagua [c], Glenn Alea [c]

[a] Physics Department, De La Salle University, Manila 0922, Philippines
[b] Centre of Excellence for Biomass Utilization, Taiwan-Malaysia Innovation Center for Clean Water and Sustainable Energy (WISE Center), Universiti Malaysia Perlis (UniMAP), Kompleks Pusat Pengajian Jejawi 2, Taman Muhibbah, 02600 Arau, Perlis, Malaysia
[c] Chemistry Department, De La Salle University, Manila 0922, Philippines
[d] School of Materials Engineering, Universiti Malaysia Perlis (UniMAP), Kompleks Pusat Pengajian Jejawi 2, Taman Muhibbah, 02600 Arau, Perlis, Malaysia

ARTICLE INFO

Keywords:
Theoretical chemistry
Pyrazinamide
Tuberculosis
Density functional theory
Bioactivity
Chemical reactivity

ABSTRACT

Conventional drugs used to treat Tuberculosis (TB) are becoming ineffective due to the occurrence of multiple drug resistant strains of tuberculosis (TB). This has made the TB disease a a serious global health dilemma. Hence, there is desperate necessity for the advancement of new drugs. In this work, the chemical reactivity and bioactivity of several analogs ofpyrazinamide (PZA) were investigated. PZA is one of the first-line of drugs used to treat tuberculosis and is a key contributor to shortening the treatment time for the disease. Chemical reactivity descriptors of pyrazinamide (PZA) and its analogs of acetylsalicyclic acid and salicyclic acid were investigated using conceptual density functional theory in water as a solvent at the MN12SX/Def2TZVP level of theory. Results have shown that all PZA analogs have improved their global and local reactivity indeces as compared to pyrazinamide based on its electronegativity, electrodonating power, electroaccepting power, eletrophilicity, global hardness and dual descriptor condensed fukui indexes. Moreover, their pKa values are slightly higher than PZA. In terms of its drug-likeness, all PZA analogs passed the Lipinski's Rule of Five criteria. Furthermore, their bioactivity scores are significantly better than pyrazinamide indicating good reaction to G-Protein Coupled Receptor (GPCR) ligands, kinase inhibitors, ion channel modulators, nuclear receptor ligands, protease inhibitors and other enzyme targets. Overall, the PZA analogs are found to be promising anti-tuberculosis drugs. Based on global and local reactivity descriptors, pKa and bioactivity scores, PZA analog of *5-n-Octanoylsalicylic acid* is the most reactive among the PZA analogs tested.

1. Introduction

Tuberculosis is now ranked above HIV, as a leading cause of death worldwide from a single infectious agent [1]. It is caused by *Mycobacterium tuberculosis (Mtb)*, which may be acquired through the ambient air upon interaction with people that expel the bacteria by coughing [2].

In the global tuberculosis report of 2019 published by the World Health Organization (WHO), data shows that the goals set for the 2020 milestones of the End TB Strategy are far from being met. The goal was to reach a 20% cumulative reduction of TB incidence by 2020 but only a 6.3% reduction was achieved from 2015-2018. This is also seen in the % reduction of TB deaths which was just 11% (between 2015 - 2018) falling short from the expected 35% reduction [1].

Research on discovering new medicinal drugs to treat tuberculosis has grown and has led to the synthesis of new chemical analogs based on the current first line of anti-tuberculosis drugs. This is mainly due to the occurrence of multiple drug resistant strains of *Mycobacterium tuberculosis*. Multi-drug resistant tuberculosis (MDR-TB) is acquired when the infection is due to the strain of TB bacteria being resistant towards any of the first line of drugs (i.e. pyrazinamide, isoniazid, ethambutol and rifampin). This threatens the effectivity of the chemotherapy regiment for the current treatment [3, 4]. A total of 186, 772 cases of MDR-TB cases were detected in 2018. In the Philippines, around 18,000 incident cases of MDR-TB were reported in 2018 from the 591,000 total TB incident cases. Tuberculosis is level 3 dangerous infectious diseases which means providing an effective therapy is a necessity [1, 5].

* Corresponding author.
E-mail address: arcvillagracia@gmail.com (A.R. Villagracia).

https://doi.org/10.1016/j.heliyon.2020.e04239
Received 20 May 2020; Received in revised form 4 June 2020; Accepted 15 June 2020

Among the first-line of anti-TB drugs, pyrazinamide (PZA) is found to be an essential sterilizing drug which shortens the tuberculosis therapy. Studies have shown that PZA disrupts the membrane energetics when the PZA drug is processed by pyrazinamidase (PZAse) to form pyrazinoic acid (POA) inside the MTB cell [6]. This allows the other anti-TB drugs to become more effective in treating tuberculosis. The occurrence of resistant strains towards the PZA drug contributes to further challenges in the treatment process. One of the known mechanisms of PZA resistance is due to mutations on the *pncA* gene which codes for the PZAse enzyme (converts PZA to its active POA form) [3]. Almost 70–97% of isolated resistant strains of *Mtb* has observed mutations for the *pncA* gene but the other 3–30% have mutations [7, 8] on other variants of the *pncA* gene and other genes like *rpsA* and *panD* which are related to the other modes of action of PZA. Inclusion of the PZA drug to fluoroquinolone treatment regimens for patients with MDR-TB, found that it improved treatment success by 38%. This was also previously seen in a study done for a mouse model which showed the enhanced activities for the second-line of drugs which included PZA than those that did not [3]. In response to the occurrence of PZA resistant strains, Alea et al. (2017) synthesized several pyrazinamide analogs of salicylic acid and acetylsalicylic acid. They have characterized the compounds through infrared spectroscopy, high-resolution mass spectrometry, and ^{1}H-NMR spectroscopy. However, no chemical reactivity studies were done [4].

Conceptual density functional theory (DFT) [9, 10] calculations allows the measurement of the chemical reactivity of molecules. This is one of the tools used in the pharmaceutical industry for drug discovery. Numerous literatures have used DFT to measure the reactivity of pyrazinamide analogs with peptides [11, 12]. In this work, the chemical reactivity of pyrazinamide and its analogs were evaluated using conceptual density functional theory through global and local reactivity descriptors, fukui functions, and pKas. Furthermore, the bioactivity properties of PZA and its analogs with G-Protein Coupled Receptor (GPCR) ligands, kinase inhibitors, ion channel modulators, nuclear receptor ligands, and protease inhibitors were also determined.

2. Materials and methodology

2.1. Calculation details

All quantum calculations implementing density functional theory were performed using PC-GAMESS/Firefly QC package, which is partly based on GAMESS (US) source code [13, 14]. The screen exchange functional Minnesota 12 (MN12-SX) [15] was used to approximate the exchange-correlation energy which uses about 25% of the exact Hartree-Fock (HF) exchange for short range and 0% HF exchange for long range and a valence triple-zeta polarization (def2-TZVP) [16] as the basis set which satisfactorily predicts trends in organic matters [17]. All atoms were geometrically relaxed and conformer search was performed filtering up to fifty conformers with the lowest ground state energy with a tolerance value of 0.0001 Ha/Bohr in water as a solvent.

Furthermore, the bioactivity prediction online-site Molinspiration Cheminfomatics has been used to determine the bioactivity scores based on the previous studies [18, 19, 20]. It calculates the LogP, molecular polar surface area, rule of five, and number of rotatable bonds. It provides the drug-likeness scores which predicts possible binding or docking to G-Protein Coupled Receptor (GPCR) ligands, kinase inhibitors, ion channel modulators, nuclear receptor ligands, protease inhibitors and other enzyme targets.

2.2. Molecular structures

The chemical reactivities of pyrazinamide and four of its analogs using salicylic and acetylsalicylic acid were determined in this study as shown in Figure 1. The PZA analogs of salicylic acid are SAL_5a (PZA analog of *5-n-Octanoylsalicylic acid* or *2-hydroxy-5-(1-(2-(pyrazine-2-*

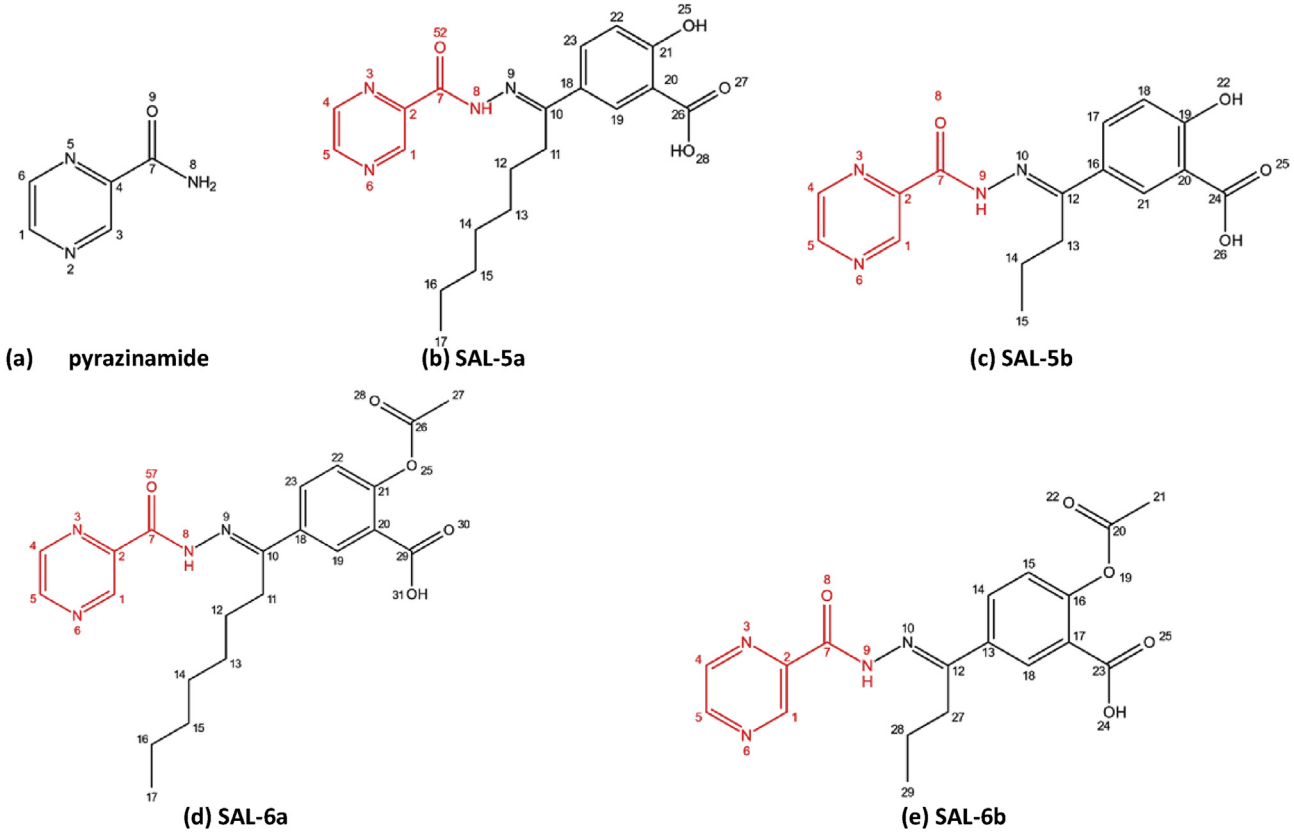

Figure 1. Pyrazinamide and its analogs.

carbonyl)hydrazineylidene)octyl)benzoic acid, Figure 1b) and SAL_5b (PZA analog of *5-n-Butanoylsalicylic acid* (5b) or *2-hydroxy-5-(1-(2-(pyrazine-2-carbonyl)hydrazineylidene)butyl) benzoic acid,* Figure 1c). These were synthesized by attaching an 8 carbon and a 4 carbon acyl chain respectively on the salicylic acid molecule, followed by coupling it with PZA via an imine bond formation [4].

The PZA analogs of acetylsalicylic acid are: SAL_6a (PZA analog of *5-n-Octanoylacetylsalicylic acid* (*2-acetoxy-5-(1-(2-(pyrazine-2-carbonyl) hydrazineylidene)octyl)benzoic acid,* Figure 1d) and SAL_6b (PZA analog of *5-n-Butanoylacetylsalicylic acid* (*2-acetoxy-5-(1-(2-(pyrazine-2-carbonyl) hydrazineylidene)butyl)benzoic acid,* Figure 1e) The red groups on Figure1b-1e corresponds to the pyrazinamide component of each molecule.

2.3. Properties and reactivity descriptors

The frontier orbitals of 50 conformer molecules with the lowest energies of each pyrazinamide analogue were computed. In this work, a Koopmans in DFT (KID) technique [21] was implemented by calculating the global reactivity descriptors based on the highest occupied molecular orbital or HOMO ($\in_H$) and lowest unoccupied molecular orbital or LUMO ($\in_L$) energies as derived using the finite difference approximation [22]:

2.3.1. Electronegativity

Electronegativity indicates the tendency of an atom to attract electrons in a molecule [23]. When electronegativity is high, there will be a full transfer of electron from the unfilled valence shell of one atom to the unfilled shell of another atom. This can lead to instability of a molecule. The electronegativity is computed as:

$$\textbf{Electronegativity}\ (\chi) \approx -\frac{1}{2}(\in_L + \in_H) \tag{1}$$

Kobayashi et al. (1998) established that electronegativity plays an important role as a factor of bioactivity in the structure-activity relationship [24].

2.3.2. Global hardness

The hardness for acid indicates more reactivity with hard bases. Hard acids are small size molecule with more positive charge and low polarizability while hard bases contain high electronegativity, difficulty to oxidize with low polarizability [22]. This is a measurement of deformation resistance of electron density. This is computed as:

$$\textbf{Global Hardness}\ (\eta) \approx (\in_L - \in_H) \tag{2}$$

2.3.3. Electrophilicity

The electrophilicity measures the tendency of the molecule to accept electron due to their lack of electrons which is a similar concept in Lewis acid [25].

$$\textbf{Electrophilicity}\ (\omega) \approx \frac{(\in_L + \in_H)^2}{4(\in_L - \in_H)} \tag{3}$$

2.3.4. Electrodonating power, electroaccepting power, net electrophilicity

These properties were derived from the second-order Taylor series expansions of the energy as a function of the number of electrons when the molecule under electron bath [26].

$$\textbf{Electrodonating Power}\ (\omega^-) \approx \frac{(\in_L + 3\in_H)}{16\eta} \tag{4}$$

$$\textbf{Electroaccepting Power}\ (\omega^+) \approx \frac{(3\in_L + 3)}{16\eta} \tag{5}$$

$$\textbf{Ne tElectrophilicity}\ (\Psi) \approx \omega^+ + \omega^- \tag{6}$$

2.3.5. Fukui functions local reactivity descriptors for lowest energy systems

The local reactivity descriptors for each atom were computed and given as [27]:

$$\text{Nucleophilic Fukui Function}\ (f+(\mathrm{r})) = \rho_{N+1}(\mathrm{r}) - \rho_N(\mathrm{r}) \tag{7}$$

$$\text{Electrophilic Fukui Function}\ (f-(\mathrm{r})) = \rho_N(\mathrm{r}) - \rho_{N-1}(\mathrm{r}) \tag{8}$$

where N, ρ_{N+1}, and ρ_{N-1} are the electron densities of atoms that are neutral, one excess electron, and one deficit electron, respectively.

2.3.6. Acid dissociation constant

The acid dissociation constant (Ka) measures the acidic strength in a solution. A lower value of its negative log (pKa) indicates stronger

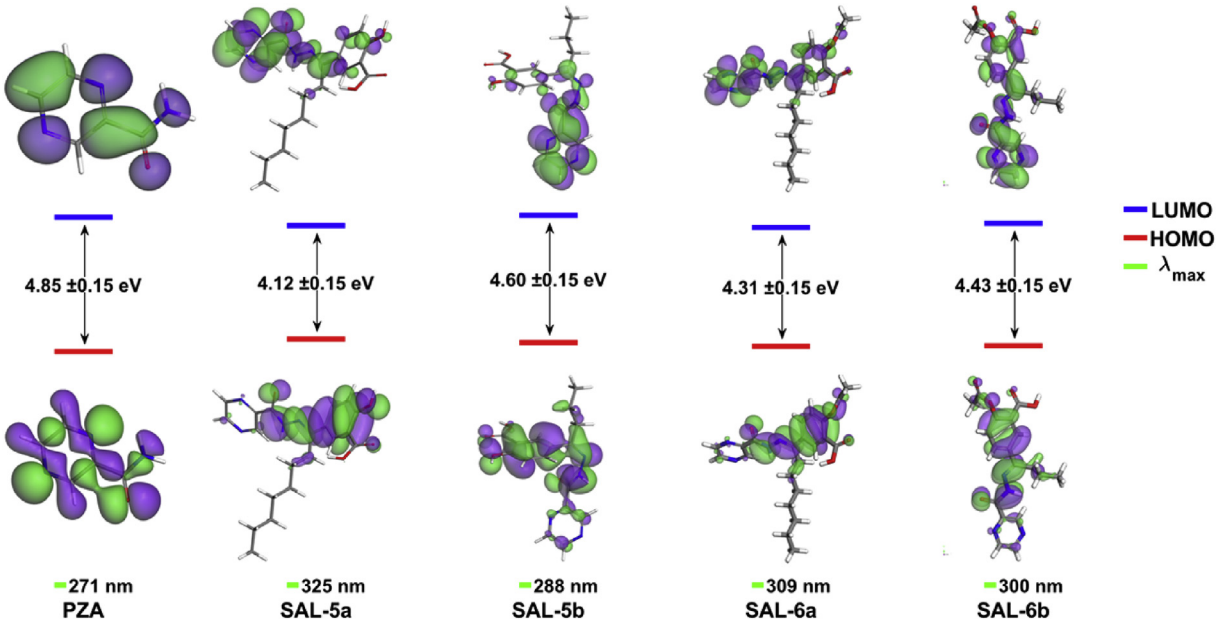

Figure 2. Ground state structures with their HOMO-LUMO orbital isosurface (isovalue: 0.02), energies and (λ_{max}).

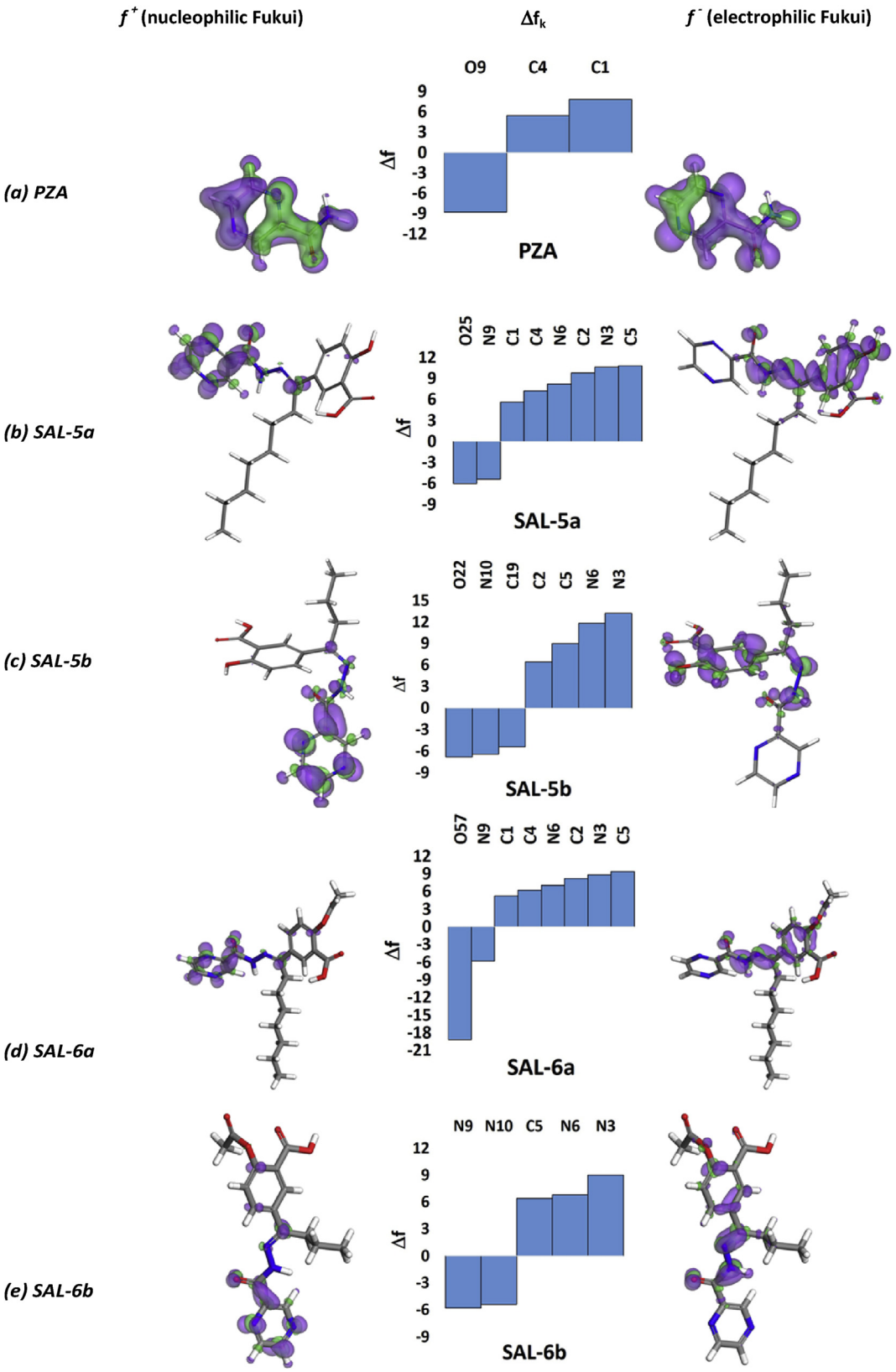

Figure 3. Fukui Function surfaces (isovalue: 0.02), left side is f^+ (nucleophilic Fukui), right is f^- (electrophilic Fukui). All values of Δf_k are multiplied by 100 for comparison purposes with a minimum absolute value of 5.

acid, consequently, it fully dissociates in water. Thus, the pKa value for peptides represents an essential role in the manufacture of medical drugs [28]. It was found that the pKa has a linear relationship using the reactivity descriptors which is given by the equation [11]:

$$\mathbf{pKa} = 16.3088 – 0.8268\boldsymbol{\eta} \quad (9)$$

2.3.7. Molecular absorption wavelength

The wavelength of maximum absorption (λ_{max}) determines the wavelength for light absorption of each molecule which can cause medicinal drug degradation. This information can aid in experimental characterization in determining the analyte concentration in each sample using Beer-Lambert Law. This is inversely proportional to the hardness of the molecule, and computed as [29]:

$$\lambda_{max} \approx 1240 / |\in_L - \in_H| \quad (10)$$

3. Result and discussion

A statistical significance test (p-value < 0.05) were performed for each reactivity descriptor using the frontier orbitals of fifty conformer molecules with the lowest energies.

3.1. HOMO-LUMO energies and maximum absorption wavelength

The HOMO-LUMO energies are shown in Figure 2. The HOMO-LUMO energies of pyrazinamide were comparable with the results of the previous study [30]. Consequently, the computed reactivity descriptors and maximum absorption wavelength agrees as well. The maximum absorption wavelengths were computed based on the lower limit of the HOMO-LUMO gap.

The HOMO-LUMO gap for the pyrazinamide analogs were lower than that of the PZA molecule, while their maximum absorption wavelengths were higher than PZA. It is noticeable that the LUMO orbitals of all analogs were found in the pyrazinamide substituent. This is indicative that that it has remained to be a good location for accepting electrons. On the other hand, the HOMO orbitals were found at the non—pyrazinamide constituents. The HOMO and LUMO were not found in the long carbon chains. These results agree with the computed Fukui functions which show the sites for nucleophilic or electrophilic attack as shown in Figure 3. These local descriptors show which atoms are vulnerable for an attack.

3.2. Local reactivity descriptors calculation

According to previous studies [31, 32], the Dual Descriptor (Δf_k) which is the difference between the electrophilic and nucleophilic Fukui functions, is more useful in predicting preferred sites of reaction than the Fukui functions alone. Overall, the pyrazinamide substituent in the PZA analogs, retained its tendency for nucleophilic attack, while the other regions of the PZA analogs were predicted to be prone to electrophilic attack except for the carbon tails. The pyrazinamide and SAL-6a have the same set of atoms that are most prone to nucleophilic and electrophilic attacks, respectively. However, the oxygen atom of the SAL-6a has contributed to the improvement of its reactivity for an electrophilic attack. The oxygen atoms in the hydroxyl group of SAL-5a and SAL-5b were the most prone atoms for electrophilic attack. The PZA analogs SAL-5a and SAL-6a have the greatest number of atoms that are prone to electrophilic or nucleophilic attack.

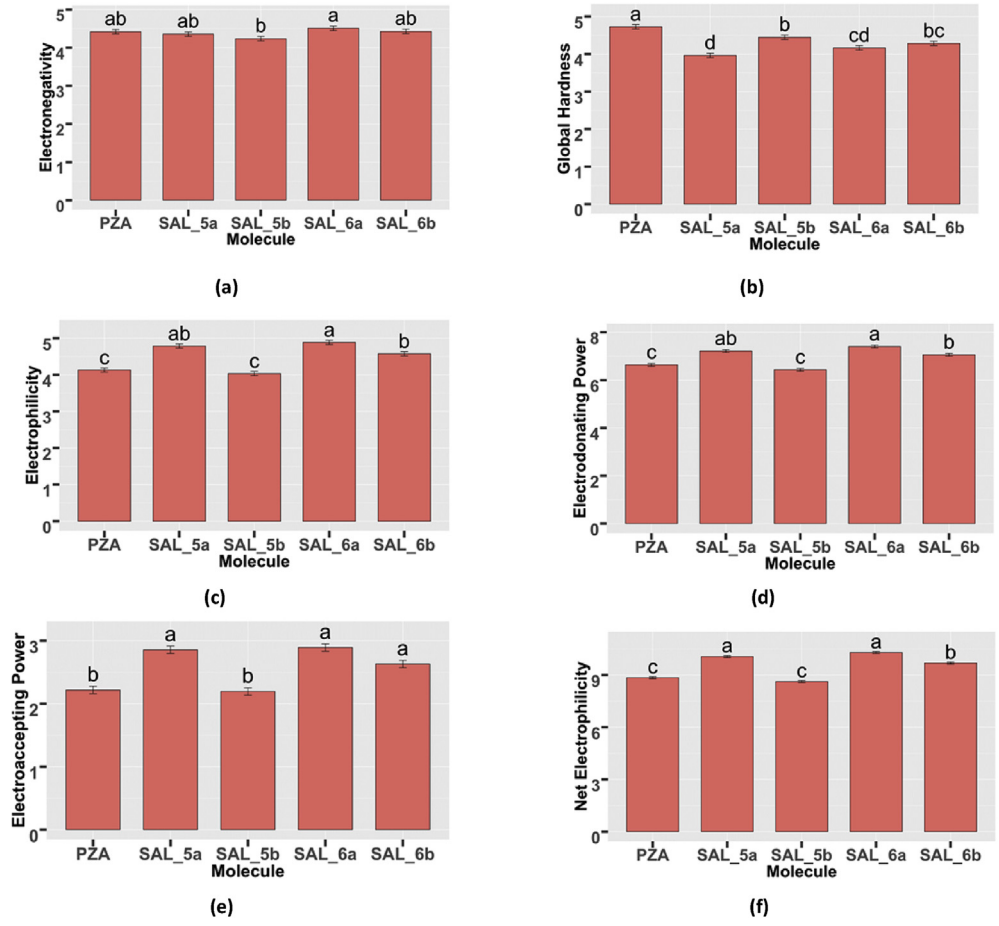

Figure 4. Global reactivity descriptors aof pyrazinamide and PZA analogs of salicylic and acetylsalicylic acids.

3.3. Global reactivity descriptors calculation

The global reactivity descriptors of the PZA analogs and its conformers were computed based on the HOMO and LUMO energies. Statistical significance tests (p-value < 0.05) were implemented to determine any significant difference between the computed properties. The significant differences were specified using alphabets to distinct one the data from group to another shown in Figure 4.

The PZA analog SAL-6a has the highest electronegativity which means it tends to attract more electrons compared to all PZA analogs and pyrazinamide. This is followed by the pyrazinamide, SAL-6b, SAL-5a, and lastly SAL-5b. The net electrophilicity values follows the trend in Electrodonating Power since it is greatly affected by the magnitude of electrodonating power values dominating the electroaccepting power. Moreover, the electrodonating power, electrophilicity and net electrophilicity have the same pattern which indicates that the PZA analog SAL-6a and SAL-5a are almost equally electrophilic followed by SAL-6b, and lastly by PZA and SAL-5b. These results show that the ability of the PZA analogs to donate and attract electrons are comparably better than the PZA specifically the PZA analogs of acetylsalicylic acid. These PZA analogs have weaker resistance to electron density deformation based on their global hardness compared to PZA. The PZA analog SAL-5a has the weakest resistance indicating higher reactivity.

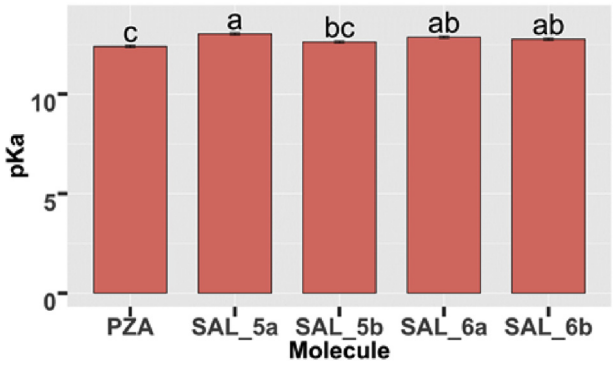

Figure 5. Global reactivity descriptors and pKa of pyrazinamide and PZA analogs of salicylic and acetylsalicylic acids.

3.4. Calculation of the pKas of the pyrazinamide and its analogs

The pKa values in Figure 5 show that the PZA analogs are slightly more soluble than pyrazinamide. The PZA analog SAL-5a is the most soluble among them followed by SAL-6a, SAL-6b, SAL-5b and lastly pyrazinamide. This result agrees with the values found in global hardness. The PZA analog SAL-5a is the most reactive among the PZA analogs. Overall, the PZA analogs are more reactive compared to PZA.

3.5. Molecular and bioactivity properties of the pyrazinamide and its analogs

The reactivity indices discussed in the previous section are based on the tendency of the molecules to accept/donate electrons, deformation of electron density and solubility. In the bioactivity properties approximation, the drug-likeness normally follows the Lipinski Rule of Five [18, 33] which determines the degree of oral bioavailability of molecules. The Rule of Five states that the molecule should have no more than five hydrogen bond donors, no more than 10 hydrogen bond acceptors, a molecular mass less than 500 Da, and an octanol-water partition coefficient (logP) not exceeding a value of 5. Table 1 shows the results for theses molecular properties. All PZA analogs passed the Lipinski Rule of Five, indicating that they are potential drug molecules. Attaching the pyrazinamide moeity to salicylic and acetylsalicylic acid which belong to the class of aspirin drugs resulted to drug-likeness.

Table 1. Molecular properties.

Property	PZA	SAL-5a	SAL-5b	SAL-6a	SAL-6b
LogP	-0.71	4.54	2.52	4.10	2.08
Topological Polar Surface Area	68.88	124.77	124.77	130.85	130.85
Molecular weight	123.11	384.44	328.33	426.47	370.37
Lipinksi's Rule Violations	0	0	0	0	0
Rotatable Bonds	1	10	6	12	8
Volume	106.00	354.18	286.97	390.69	323.48

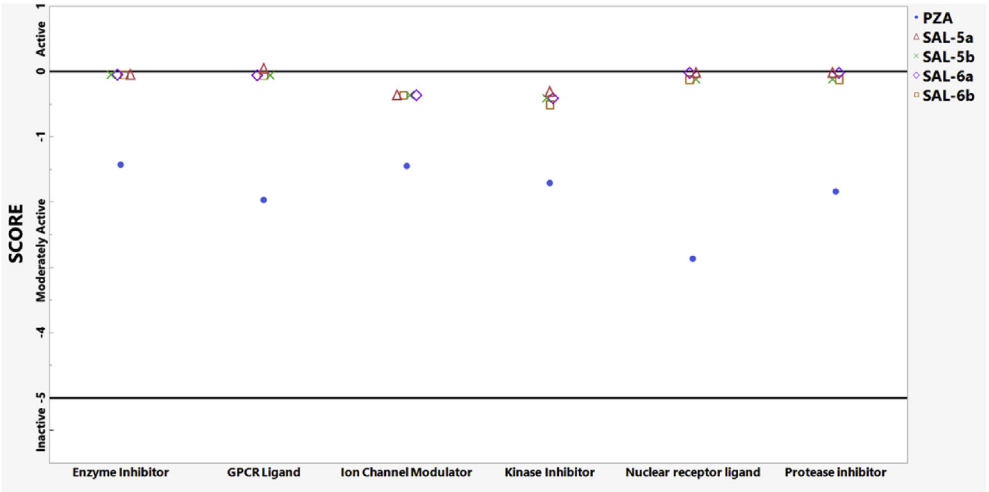

Figure 6. Bioactivity properties of PZA and its analogs.

Previous works [11, 34, 35, 36] have used Molinspiration to provide the bioactivity properties. Figure 6 shows the bioactivity properties of the PZA analogs to a library of GPCR ligand, enzyme inhibitor, protease inhibitor, nuclear receptor ligand, kinase inhibitor and ion channel modulator.

In Figure 6, the molecules whose bioactivity scores were greater than or equal to zero were classified to be active. To be considered moderately active, the bioactivity score should be between zero and negative five, while scores less than negative five are categorized as inactive.

The pyrazinamide molecule and all PZA analogs were found to be moderately active, while all PZA analogs are very close to the region of active. This indicates that the PZA analogs are more bioactive compared to pyrazinamide. Moreover, the PZA analog SAL-5a has a bioscore of 0.0 for GPCR ligand which can be classified to be active. The results have shown that all PZA analogs were potential drugs for tuberculosis based on the reactivity, solubility, and bioactivity.

4. Conclusions

The chemical reactivity of pyrazinamide analogs of salicyclic and acetylsalicyclic acid [4] were calculated using conceptual density functional theory, while its molecular and bioactive properties were determined using Lipinski Rule of Five and Molinspiration. Results have shown that all PZA analogs improved their capacity to donate and accept electrons, they have weaker resistance to electron density deformation with comparable pKa to PZA, and they all passed the Rule of Five drug-likeness test and gave better bioactivity towards the GPCR ligand, as an enzyme inhibitor, a protease inhibitor, a nuclear receptor ligand, a kinase inhibitor and an ion channel modulator. These results indicate that all PZA analogs have the great potential to be an anti-tuberculosis agent with better reactivity compared to PZA alone. Among the PZA analogs, SAL-5a was found to be the most reactive based on its global and local reactivity descriptors, pKa and bioactivity scores.

Declarations

Author contribution statement

Al Rey Villagracia: Conceived and designed the experiments; Performed the experiments; Analyzed and interpreted the data; Contributed reagents, materials, analysis tools or data; Wrote the paper.

Hui Lin Ong: Conceived and designed the experiments; Analyzed and interpreted the data; Contributed reagents, materials, analysis tools or data; Wrote the paper.

Faith Marie Lagua, Glenn Alea: Analyzed and interpreted the data; Contributed reagents, materials, analysis tools or data; Wrote the paper.

Funding statement

This research did not receive any specific grant from funding agencies in the public, commercial, or not-for-profit sectors.

Competing interest statement

The authors declare no conflict of interest.

Additional information

No additional information is available for this paper.

Acknowledgements

We would like to thank the University Research Coordination Office and the Office of the Vice Chancellor of Research and Innovation, and Physics Department of De La Salle University.

References

[1] WHO, WHO | Global Tuberculosis Report 2019, 2020.
[2] Y. Zhang, M.M. Wade, A. Scorpio, H. Zhang, Z. Sun, Mode of action of pyrazinamide: disruption of Mycobacterium tuberculosis membrane transport and energetics by pyrazinoic acid, J. Antimicrob. Chemother. 52 (5) (2003) 790–795.
[3] M. Njire, Y. Tan, J. Mugweru, C. Wang, J. Guo, W.W. Yew, S. Tan, T. Zhang, Pyrazinamide resistance in Mycobacterium tuberculosis: review and update, Adv. Med. Sci. (2016) 63–71. Medical University of Bialystok March 1.
[4] G.V. Alea, F.M.G. Lagua, M.D.M. Ajero, Synthesis and characterization of pyrazinamide analogs of acetylsalicylic acid and salicylic acid, Philipp. J. Sci. 146 (4) (2017) 457–468.
[5] L.V. White, T. Edwards, N. Lee, M.C. Castro, N.R. Saludar, R.W. Calapis, B.N. Faguer, N. Dela Fuente, F. Mayoga, N. Saito, K. Ariyoshi, A.M.C.G. Garfin, J.A. Solon, S.E. Cox, Patterns and predictors of Co-morbidities in tuberculosis: a cross-sectional study in the Philippines, Sci. Rep. 10 (1) (2020) 4100.
[6] H. Sayahi, O. Zimhony, W.R. Jacobs, A. Shekhtman, J.T. Welch, Pyrazinamide, but not pyrazinoic acid, is a competitive inhibitor of NADPH binding to Mycobacterium tuberculosis fatty acid synthase I, Bioorg. Med. Chem. Lett 21 (16) (2011) 4804–4807.
[7] M. Karmakar, C.H.M. Rodrigues, K. Horan, J.T. Denholm, D.B. Ascher, Structure guided prediction of pyrazinamide resistance mutations in PncA, Sci. Rep. 10 (1) (2020) 1–10.
[8] N. T. Le Hang, M. Hijikata, S. Maeda, P.H. Thuong, J. Ohashi, H. Van Huan, N.P. Hoang, A. Miyabayashi, V.C. Cuong, S. Seto, N. Van Hung, N. Keicho, Whole genome sequencing, analyses of drug resistance-conferring mutations, and correlation with transmission of Mycobacterium tuberculosis carrying KatG-S315T in Hanoi, Vietnam. *Sci. Rep.* 9 (1) (2019) 1–14.
[9] P. Geerlings, F. De Proft, W. Langenaeker, Conceptual density functional theory, Chem. Rev. 103 (5) (2003) 1793–1873.
[10] R.G. Parr, Density functional theory of atoms and molecules, in: Horizons of Quantum Chemistry, Springer Netherlands, 1980, pp. 5–15.
[11] N. Flores-Holguín, J. Frau, D. Glossman-Mitnik, Chemical reactivity and bioactivity properties of the phallotoxin family of fungal peptides based on conceptual peptidology and DFT study, Heliyon 5 (8) (2019), e02335.
[12] T. Bettens, M. Alonso, P. Geerlings, F. De Proft, The hunt for reactive alkynes in bio-orthogonal click reactions: insights from mechanochemical and conceptual DFT calculations, Chem. Sci. 11 (2020) 1431–1439.
[13] M.W. Schmidt, K.K. Baldridge, J.A. Boatz, S.T. Elbert, M.S. Gordon, J.H. Jensen, S. Koseki, N. Matsunaga, K.A. Nguyen, S. Su, T.L. Windus, M. Dupuis, J.A. Montgomery, General atomic and molecular electronic structure system, J. Comput. Chem. 14 (11) (1993) 1347–1363.
[14] A. Granovsky, GAMESS/Firefly, *GAMESS/Firefly*, 2013. http://classic.chem.msu.su/gran/gamess/index.html.
[15] R. Peverati, D.G. Truhlar, Screened-exchange density functionals with broad accuracy for chemistry and solid-state Physics, Phys. Chem. Chem. Phys. 14 (47) (2012) 16187–16191.
[16] K. Kirschner, D. Reith, W. Heiden, The Performance of Dunning, Jensen and Karlsruhe Basis Sets on Computing Relative Energies and Geometries, 2019.
[17] J. Tirado-Rives, W.L. Jorgensen, Performance of B3LYP density functional methods for a large set of organic molecules, J. Chem. Theor. Comput. 4 (2) (2008) 297–306.
[18] C.A. Lipinski, F. Lombardo, B.W. Dominy, P.J. Feeney, Experimental and computational approaches to estimate solubility and permeability in drug discovery and development settings, Adv. Drug Deliv. Rev. 46 (1–3) (2001) 3–26.
[19] D.F. Veber, S.R. Johnson, H.-Y. Cheng, B.R. Smith, K.W. Ward, K.D. Kopple, Molecular properties that influence the oral bioavailability of drug candidates, J. Med. Chem. 45 (12) (2002) 2615–2623.
[20] P. Ertl, B. Rohde, P. Selzer, Fast calculation of molecular polar surface area as a sum of fragment-based contributions and its application to the prediction of drug transport properties, J. Med. Chem. 43 (20) (2000) 3714–3717.
[21] T. Koopmans, Über die Zuordnung von Wellenfunktionen und eigenwerten Zu den einzelnen elektronen eines atoms, Physica 1 (1–6) (1934) 104–113.
[22] W. Yang, R.G. Parr, Hardness, softness, and the fukui function in the electronic theory of metals and catalysis, Proc. Natl. Acad. Sci. U. S. A 82 (20) (1985) 6723–6726.
[23] R. Crichton, Biological Inorganic Chemistry, Elsevier, 2012.
[24] S. Kobayashi, H. Hamashima, M. Kurihara, N. Miyata, A. Tanaka, Hardness controlled enzymes and electronegativity controlled enzymes: role of an absolute hardness-electronegativity (η-χ) activity diagram as a coordinate for biological activities, Chem. Pharm. Bull. 46 (7) (1998) 1108–1115.
[25] C. Morell, J.L. Gázquez, A. Vela, F. Guégan, H. Chermette, Revisiting electroaccepting and electrodonating powers: proposals for local electrophilicity and local nucleophilicity descriptors, Phys. Chem. Chem. Phys. 16 (48) (2014) 26832–26842.
[26] J.L. Gázquez, A. Cedillo, A. Vela, Electrodonating and electroaccepting powers, J. Phys. Chem. 111 (10) (2007) 1966–1970.
[27] W. Yang, W.J. Mortier, The use of global and local molecular parameters for the analysis of the gas-phase basicity of amines, J. Am. Chem. Soc. 108 (19) (1986) 5708–5711.
[28] J. Frau, N. Hernández-Haro, D. Glossman-Mitnik, Computational prediction of the PKas of small peptides through conceptual DFT descriptors, Chem. Phys. Lett. 671 (2017) 138–141.
[29] Y. Zhou, Q. He, Y. Yang, H. Zhong, C. He, G. Sang, W. Liu, C. Yang, F. Bai, Y. Li, Binaphthyl-containing green- and red-emitting molecules for solution-processable organic light-emitting diodes, Adv. Funct. Mater. 18 (20) (2008) 3299–3306.

[30] A. Favila, M. Gallo, D. Glossman-Mitnik, CHIH-DFT determination of the molecular structure infrared spectra, UV spectra and chemical reactivity of three antitubercular compounds: rifampicin, isoniazid and pyrazinamide, J. Mol. Model. 13 (4) (2007) 505–518.
[31] J.I. Martínez-Araya, Why is the dual descriptor a more accurate local reactivity descriptor than fukui functions? J. Math. Chem. 53 (2) (2014) 451–465.
[32] C. Morell, A. Grand, A. Toro-Labbé, Theoretical support for using the Δf(r) descriptor, Chem. Phys. Lett. 425 (4–6) (2006) 342–346.
[33] R.J.A. Goodwin, J. Bunch, D.F. McGinnity, Mass spectrometry imaging in oncology drug discovery, in: Advances in Cancer Research, 134, Academic Press Inc., 2017, pp. 133–171.
[34] M. Jagadeb, S.N. Rath, A. Sonawane, Computational discovery of potent drugs to improve the treatment of pyrazinamide resistant Mycobacterium tuberculosis mutants, J. Cell. Biochem. 119 (9) (2018) 7328–7338.
[35] D.S. Reddy, M. Kongot, S.P. Netalkar, M.M. Kurjogi, R. Kumar, F. Avecilla, A. Kumar, Synthesis and evaluation of novel coumarin-oxime ethers as potential anti-tubercular agents: their DNA cleavage ability and BSA interaction study, Eur. J. Med. Chem. 150 (2018) 864–875.
[36] T. Khan, I. Azad, R. Ahmad, S. Raza, S. Dixit, S. Joshi, A.R. Khan, Synthesis, characterization, computational studies and biological activity evaluation of CU, FE, CO and ZN complexes with 2-butanone thiosemicarbazone and 1,10-phenanthroline ligands as anticancer and antibacterial agents, EXCLI J 17 (2018) 331–348.